Multi-Format Carrier Phase Recovery Using a Programmable Circuit

(article starts on next page)

Multi-Format Carrier Phase Recovery Using a Programmable Circuit

Erik Börjeson and Per Larsson-Edefors

Dept. of Computer Science and Engineering, Chalmers University of Technology, Gothenburg, Sweden
erikbor@chalmers.se

Abstract: We introduce an application-specific circuit that can be programmed to efficiently perform blind carrier phase recovery for different modulation formats. A circuit implementation that supports QPSK/16/32/64QAM is evaluated. © 2021 The Author(s)

1. Introduction

Tailored to DSP algorithms, application-specific integrated circuits (ASICs) offer high electrical performance. But optimizing circuits for a narrow application domain has the adverse effect that the ASIC's performance deteriorates when the system context changes. Take, for example, carrier phase recovery: For QPSK, the Viterbi-Viterbi algorithm [1] is adequate, but when used for 64QAM, the SNR penalty of this algorithm rises significantly [2], suggesting a receiver ASIC needs several different CPR circuits to support multiple modulation formats; this will waste area. Not only does the choice of algorithm depend on format, but also choice of fixed-point resolution varies [3]. The challenge we address here is how to develop one single versatile CPR circuit that can provide high performance and high energy efficiency in a range of systems, from QPSK to 64QAM and including 32QAM.

2. Circuit Implementation

Based on the work done in [3] and [4], we have identified principal component-based phase estimation (PCPE) [5] to be a good choice for a multi-format CPR implementation, as it can handle multiple square QAM formats without any modification. Other popular algorithms, such as blind phase search [6] or versions of the Viterbi-Viterbi estimator [2], need larger circuit extensions to support multiple formats, resulting in a larger total area.

A schematic of our multi-format CPR circuit is shown in Fig. 1. To support 30 GBd, we parallelize the circuit in $P = 32$ lanes and use a clock rate of 938 MHz. The circuit is programmable with logic signals, which define the current modulation format and window size. When using lower-order formats, the input signal wordlength needed to perform CPR is typically reduced; this can be used to minimize the circuit switching activity and power dissipation. But in a multi-format circuit, the wordlength of all internal signals has to be set to support the highest-order format needed. The *control* module then is used to create bit masks that reduce the number of bits utilized for the lower-order formats by setting the least significant bits to zero. Fig. 2 shows two ways that this mask is used to control the switching activity, where the top version is used for registers, i.e., clock gating. For the intermediate logic we use the bottom version, where an AND gate is used to mask the switching, preventing the signal to propagate further. The small delay introduced by the extra gate is negligible compared to the rest of the data path.

To perform CPR also for the non-square 32QAM format, we add the *magnitude scaling* module, which compares the input symbols to a set limit to detect the innermost ring in the constellation, using the approximation $\max\left(\Re(x), \Im(x)\right) + \frac{1}{2}\min\left(\Re(x), \Im(x)\right) < L$, where x is the input symbol and L is a modulation-format-dependent magnitude limit. The symbols in this ring are amplified by left-shifting, which makes phase recovery possible also for 32QAM. This method has the added benefit of reducing the SNR penalty for both 16QAM and 64QAM. The mask and other control signals are generated and synchronized to the DSP pipeline in the *control* module, which also controls the window size, *A*, for the covariance calculation, making it possible to optimize the processing for different laser linewidths [4]. To reduce circuit complexity, the *A* setting is limited to multiples of *P*.
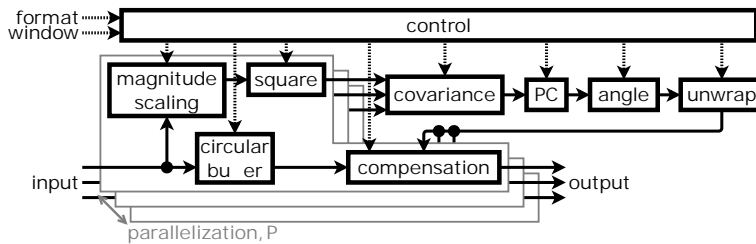

Fig. 1: Block diagram of the multi-format CPR circuit, where solid lines indicate data signals and dotted lines show control signals.
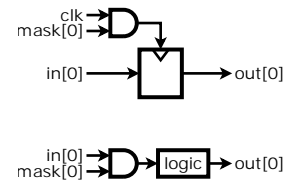

Fig. 2: Simplified schematics of the logic used to reduce switching activity.
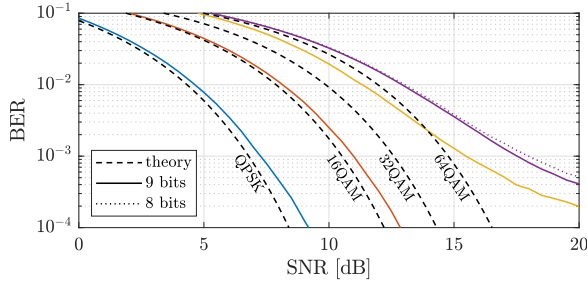
Format	Window size, A			
	32	64	96	128
QPSK	75 (1.25)	70 (1.17)	68 (1.14)	66 (1.12)
16QAM	103 (0.86)	93 (0.77)	91 (0.76)	89 (0.74)
32QAM	106 (0.71)	92 (0.61)	91 (0.61)	88 (0.59)
64QAM	115 (0.64)	103 (0.57)	100 (0.55)	100 (0.55)

Fig. 3: BER as a function of SNR for a 30-GBd circuit implementation using a laser linewidth of 200 kHz and $A = 96$.

Table 1: Power dissipation and energy per bit [mW (pJ/bit)] for a 9-bit 30-GBd multi-format CPR circuit.

3. Results

System simulations were done using a software model of our circuit and a MATLAB generated input channel with AWGN and phase noise, which is emulated as a Weiner process. The BER as a function of SNR is shown in Fig. 3 together with the theoretical minimum BER using an AWGN-only channel. These simulations assume a combined laser linewidth of 200 kHz, which corresponds to two relatively standard external-cavity lasers, resulting in an optimum setting of the covariance window of $A = 96$. The SNR penalty at a BER of 10^{-2}, approximating the soft-decision FEC limit, is slightly smaller than our previously shown results for 16QAM and 64QAM [3], thanks to the introduction of magnitude scaling. The penalty for 32QAM is higher than for the other formats, due to the lack of corner points in the constellation. However, without magnitude scaling, the added penalty would be greater than 2 dB. We select the effective wordlength for each modulation format as the point where adding additional bits do not significantly improve the SNR penalty: These are 5, 8, 8, and 9 bits for QPSK, 16QAM, 32QAM, and 64QAM, respectively. Decreasing the circuit wordlength from 9 to 8 bits only affects 64QAM with an additional penalty of 0.16 dB, since the other effective wordlengths stay constant thanks to gated signals. The 8-bit option can be useful in systems having 32QAM as the largest constellation size.

The circuit was implemented in 22 nm CMOS, assuming a 0.72-V supply voltage, 120°C, and slow process corners, to get somewhat conservative results. The resulting cell areas were 0.071 and 0.084 mm² for the 8- and 9-bit multi-format CPR circuits, respectively. This means a 9-bit multi-format circuit is 50% larger than a single-format 64QAM PCPE circuit with $A = 96$ [3]; this is due mainly to the logic added to support larger windows.

The circuit netlist was simulated using varying modulation formats, and the resulting switching statistics were used for power analysis, using 0.8 V, 85°C, and typical corners. The power results are shown in Table 1. Compared to single-format 16QAM and 64QAM PCPE, the power overhead for the multi-format approach is only between 8 and 14%; this is because clock and signal-gating techniques are efficient in reducing power dissipation when lower-order formats are used. For systems employing lasers with lower linewidths, larger window sizes can be used, which further increases the potential of clock gating due to less frequent updates of the estimated phase.

4. Conclusion

We have shown a multi-format principal component-based phase estimator (PCPE) circuit that can be programmed to support modulation formats ranging from QPSK to 64QAM. The programming can be performed at deployment or during processing, offering the possibility to dynamically adjust the format depending on the quality of the transmission. This circuit uses extensive gating of clock and data signals to reduce power dissipation for modulation formats that do not need the full resolution of the circuit, which results in a power dissipation just 8–14% higher than corresponding single-format PCPE implementations. We also show how magnitude scaling can be used to facilitate the utilization of PCPE also for non-square modulation formats, such as 32QAM, further broadening the potential usage of the circuit.

References

[1] A. J. Viterbi and A. M. Viterbi, "Nonlinear estimation of PSK-modulated carrier phase with application to burst digital transmission," IEEE Transactions on Information Theory 29, 543–551 (1983).

[2] S. M. Bilal *et al.*, "Multistage carrier phase estimation algorithms for phase noise mitigation in 64-quadrature amplitude modulation optical systems," Journal of Lightwave Technology 32, 2973–2980 (2014).

[3] E. Börjeson and P. Larsson-Edefors, "Benchmarking of carrier phase recovery circuits for *M*-QAM coherent systems," in "OFC," (2021).

[4] E. Börjeson and P. Larsson-Edefors, "Energy-efficient implementation of carrier phase recovery for higher-order modulation formats," Journal of Lightwave Technology 39, 505–510 (2021).

[5] J. C. M. Diniz *et al.*, "Low-complexity carrier phase recovery based on principal component analysis for square-QAM modulation formats," Optics Express 27, 15,617–15,626 (2019).

[6] T. Pfau, S. Hoffmann, and R. Noe, "Hardware-efficient coherent digital receiver concept with feedforward carrier recovery for M-QAM constellations," Journal of Lightwave Technology 27, 989–999 (2009).